

Emission of electron Bernstein waves in plasmas

A. K. Ram, A. Bers, and C. N. Lashmore-Davies

Citation: *Phys. Plasmas* **9**, 409 (2002); doi: 10.1063/1.1429634

View online: <http://dx.doi.org/10.1063/1.1429634>

View Table of Contents: <http://pop.aip.org/resource/1/PHPAEN/v9/i2>

Published by the [American Institute of Physics](#).

Related Articles

The effects of neutral gas heating on H mode transition and maintenance currents in a 13.56MHz planar coil inductively coupled plasma reactor

Phys. Plasmas **19**, 093501 (2012)

Collisionless inter-species energy transfer and turbulent heating in drift wave turbulence

Phys. Plasmas **19**, 082309 (2012)

Development of a low-energy and high-current pulsed neutral beam injector with a washer-gun plasma source for high-beta plasma experiments

Rev. Sci. Instrum. **83**, 083504 (2012)

A stochastic mechanism of electron heating

Phys. Plasmas **19**, 082506 (2012)

Toroidal ripple transport of beam ions in the mega-ampère spherical tokamak

Phys. Plasmas **19**, 072514 (2012)

Additional information on *Phys. Plasmas*

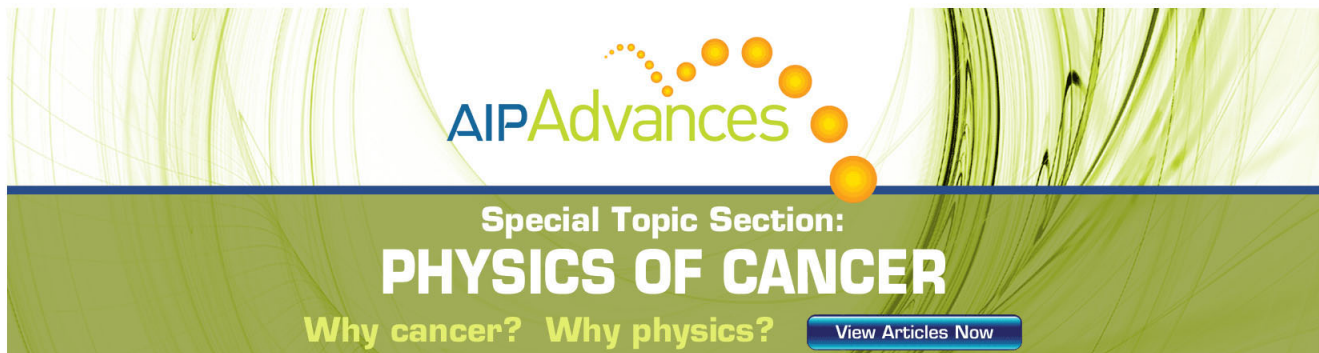
Journal Homepage: <http://pop.aip.org/>

Journal Information: http://pop.aip.org/about/about_the_journal

Top downloads: http://pop.aip.org/features/most_downloaded

Information for Authors: <http://pop.aip.org/authors>

ADVERTISEMENT



AIP Advances

Special Topic Section:
PHYSICS OF CANCER

Why cancer? Why physics? [View Articles Now](#)

Emission of electron Bernstein waves in plasmas

A. K. Ram^{a)} and A. Bers

Plasma Science and Fusion Center, Massachusetts Institute of Technology, Cambridge, Massachusetts 02139

C. N. Lashmore-Davies

Culham Science Center, UKAEA/EURATOM Fusion Association, Abingdon, Oxon OX14 3DB, United Kingdom

(Received 28 August 2001; accepted 19 October 2001)

In previous publications [A. K. Ram and S. D. Schultz, *Phys. Plasmas* **7**, 4084 (2000); A. Bers, A. K. Ram, and S. D. Schultz, in *Proceedings of the Second Europhysics Topical Conference on RF Heating and Current Drive of Fusion Devices*, edited by J. Jacquinot, G. Van Oost, and R. R. Weynants (European Physical Society, Petit-Lancy, 1998), Vol. 22A, pp. 237–240] it has been shown that, in overdense plasmas of the type encountered in spherical tori, electron Bernstein waves can be excited in a plasma by mode conversion of either an externally launched X mode or an O mode. The electron Bernstein waves are strongly absorbed by electrons in the region where the wave frequency matches the Doppler broadened electron cyclotron resonance frequency or its harmonics. The strong absorption also implies that electron Bernstein waves are emitted by a thermal plasma. These waves can then mode convert to the X mode and to the O mode and be observed external to the plasma. In this paper an approximate kinetic model describing the coupling between the X mode, the O mode, and the electron Bernstein waves is derived. This model is used to study the mode conversion properties of electron Bernstein wave emission from the plasma interior. It is shown, analytically and numerically, that the energy flow conversion efficiencies of the electron Bernstein wave to the X mode and to the O mode are the same as the energy flow conversion efficiency of the X mode to electron Bernstein waves and of the O mode to the electron Bernstein waves, respectively. This has important experimental consequences when designing experiments to heat overdense plasmas by electron Bernstein waves. © 2002 American Institute of Physics. [DOI: 10.1063/1.1429634]

I. INTRODUCTION

We have previously shown that high- β spherical tokamak plasmas can be heated by waves in the electron cyclotron range of frequencies by mode converting the X mode or the O mode to electron Bernstein waves (EBW) at the upper hybrid resonance (UHR).^{1,2} Since the slow branch of the X mode couples directly to EBWs, the mode conversion of the X mode to EBWs is a direct process. However, the conversion of the O mode to EBWs requires that the O mode first couple to the slow branch of the X mode. This occurs when the O mode is launched at an oblique angle relative to the total magnetic field.³ From ray tracing analysis we have also shown that EBWs are locally and strongly absorbed at the Doppler shifted electron cyclotron resonance or its harmonics. The strong and localized absorption implies that thermal emission of EBWs can occur for frequencies corresponding to the local Doppler-shifted electron cyclotron frequency. This emission then converts, at the UHR, to the X and O modes which are then observed in the vacuum region.

The excitation and emission of EBWs has been studied experimentally on the Wendelstein 7-AS.⁴ More recently, experiments on Current Drive Experiment–Upgrade (CDX–U) and National Spherical Torus Experiment (NSTX),⁵ Mega Amp Spherical Tokamak (MAST),⁶ and Madison Symmetric

Torus (MST)⁷ have observed emission of EBWs via the mode conversion process, and studied its dependence on the edge properties of the plasma.

In this paper we formulate an approximate kinetic description of the mode conversion process which includes the propagating EBWs. The model includes an approximate formulation of the EBW that describes its propagation, and coupling to the X and O modes, in the vicinity of the mode conversion region near the UHR. It describes the X – B conversion of the X mode to EBW and the O – B conversion of the O mode to EBWs. It is different from the traditional cold plasma models where the energy flow conversion coefficient to the EBW is given by the power resonantly absorbed at the UHR. We have shown that the fraction of the incoming energy flow, from either the X mode or the O mode, that is converted to EBWs is approximately the same as the power that is resonantly absorbed at the UHR in the cold plasma model. However, the cold plasma model cannot be used to study the mode conversion of emitted EBWs to the X mode and the O mode. For such studies a kinetic description of the EBW is required.

In Sec. II we give details of the kinetic full-wave model that we use to study the coupling between the X mode, the O mode, and the EBW. Using the principles of energy flow conservation and time-reversal invariance we derive, in Sec. III, the general symmetry relations between the emission and

^{a)}Electronic mail: abhay@psfc.mit.edu

excitation coefficients. We show that the fraction of the EBW energy flow that is mode converted to the X mode (emission coefficient) is the same as the fraction of the X mode energy flow that is converted to the EBWs (excitation coefficient) when the X mode is launched into the plasma. A fraction of the emitted EBW energy flow also converts to the O mode. This fraction is the same as the fraction of the O mode energy flow that is converted to the EBWs if the O mode were to be launched from the outside. Thus, the X and O mode emission coefficients are the same as the X and O mode excitation coefficients. This symmetry between the emission coefficients and the excitation coefficients is useful for designing experiments to heat and to drive plasma currents in spherical tokamaks by waves in the electron cyclotron range of frequencies. Since the sum of the X mode and O mode emission coefficients has to be less than unity, the parameter space for which the excitation coefficient from one of these modes is optimized is complementary to the parameter space for the optimum excitation coefficient for the other mode.¹ These results have important consequences for experimentally achieving optimum plasma edge parameters for the excitation of EBWs; such optimized parameters can be ascertained by monitoring the emission from EBWs. In Sec. IV we show that the numerical solutions of the model equations for the fields, discussed in Sec. II, give the same global results discussed in Sec. III.

By “emission,” we mean conversion from an EBW excited in the high-density and high-temperature region, interior to the plasma, to either an X or O mode in the low-density and low-temperature side, toward the outside of the plasma. This emission process is also directly related to noise emission in a band of frequencies from EBWs inside the plasma.

In Appendix A the differences in the approximate and exact WKB dispersion relations are elucidated for two cases: (a) $\omega_{UH} < 2\omega_c$, where ω_{UH} is upper hybrid angular frequency and ω_c is the electron cyclotron angular frequency; and (b) $\omega_{UH} > 2\omega_c$. Appendix B gives details of the boundary conditions associated with the numerical integration of the wave equations for mode conversion excitation of EBWs, and mode conversion emission of EBWs. The appendixes complement the previous studies^{1,2} on mode conversion excitation of EBWs in which these details were not elucidated.

II. APPROXIMATE KINETIC MODE CONVERSION FORMULATION

An approximate model of mode conversion from external (to the plasma) excitations of X and/or O modes to EBWs can be formulated using a cold plasma model wherein mode conversion appears as resonance absorption at the UHR inside the plasma. However, such a cold plasma model cannot be used to study the emission of X and/or O modes that are generated, via mode conversion at the UHR, by EBWs emitted from inside the plasma. (The X and O modes then become electromagnetic free-space modes outside the plasma and can be observed in experiments.) The EBWs require a kinetic description since they are not normal modes of a cold plasma. In general, a fully kinetic description of wave propa-

gation and mode conversion entails the solution of a system of integro-differential equations. This is a daunting task for a plasma in a magnetic field. For the present, by focussing on the kinetic mode of interest, the EBW, we formulate an approximate full-wave kinetic description for the propagation and mode conversion analysis of EBWs, X modes, and O modes. This kinetic description is formulated for a plasma with inhomogeneous density that is confined by an inhomogeneous and sheared magnetic field. Furthermore, since the mode conversion process, particularly in high- β spherical tori, occurs near the plasma edge, we can limit ourselves to an analysis in a slab geometry with an inhomogeneous and sheared magnetic field whose effective poloidal component is produced by currents that flow in the plasma away from the mode conversion region. Thus, the plasma in the mode conversion region is taken to be radially inhomogeneous and having no drifts.

The mode conversion description is formulated in a slab geometry in which the x direction represents the radial direction along which the plasma is inhomogeneous, the y direction represents the poloidal direction, and the z direction is the toroidal direction. The magnetic field in which the plasma is immersed is assumed to be sheared with the form

$$\vec{B}_0(x) \equiv B_y \hat{y} + B_z \hat{z} = B_0(x) \sin \Psi(x) \hat{y} + B_0(x) \cos \Psi(x) \hat{z}, \quad (1)$$

where Ψ is the angle between \vec{B}_0 and the z axis.

From the linearized continuity and (nonrelativistic) momentum equations for a cold plasma, and neglecting ion dynamics, the propagation of the X and O modes is given by Maxwell's equations for the first order fields (\vec{E}, \vec{B}) ^{1,2}

$$\nabla \times \vec{E} = i\omega \vec{B}, \quad \nabla \times \vec{B} = -i \frac{\omega}{c^2} \vec{K} \cdot \vec{E}, \quad (2)$$

where the time variation is assumed to be of the form $e^{-i\omega t}$, ω is the angular frequency of the wave, the permittivity tensor $\vec{K}(x, \omega)$ is

$$\begin{aligned} \vec{K} &= \vec{I} + \vec{\chi} = \begin{pmatrix} K_{xx} & \chi_{xy} & \chi_{xz} \\ -\chi_{xy} & K_{yy} & \chi_{yz} \\ -\chi_{xz} & \chi_{yz} & K_{zz} \end{pmatrix} \\ &\equiv \vec{I} - \frac{\omega_p^2}{\omega^2 - \omega_c^2} \begin{pmatrix} 1 & -i\omega_{cz} & i\omega_{cy} \\ i\omega_{cz} & 1 - \omega_{cy}^2 & -\omega_{cy}\omega_{cz} \\ -i\omega_{cy} & -\omega_{cy}\omega_{cz} & 1 - \omega_{cz}^2 \end{pmatrix} \end{aligned} \quad (3)$$

and \vec{I} is the second-rank identity tensor, $\omega_p(x)$ is the electron plasma angular frequency, $\omega_{cy}(x) = eB_y(x)/m_e$, $\omega_{cz}(x) = eB_z(x)/m_e$ are the electron cyclotron angular frequencies for the poloidal and toroidal fields, respectively, $\omega_c = \sqrt{\omega_{cy}^2 + \omega_{cz}^2}$, m_e is the electron mass, e is the electron charge, and c is the speed of light.

If we assume uniformity in the y and z directions so that the fields have a dependence of the form $e^{ik_y y + ik_z z}$, where k_y and k_z are the poloidal and toroidal components of the wave vector, then (2) are reduced to a set of ordinary differential

equations in x . These equations then describe the propagation of the cold plasma modes in a sheared magnetic field. These differential equations for the fields have a regular singularity at $K_{xx}=0$ corresponding to the upper hybrid resonance $\omega_{UH}=\sqrt{(\omega_p^2+\omega_c^2)}$. This singularity leads to resonance absorption, which, as shown in Ref. 1, is equivalent to the energy flow mode converted to electron Bernstein waves.

The approximate full wave kinetic field equations then follow from supplementing the cold plasma description as follows.^{1,2} A fully kinetic description involves, in general, an infinite number of modes. In order to single out the coupling of specific modes, it is expeditious to use a reduced order approximation that accounts for only the modes of interest. For our case we seek an approximate, reduced full-wave description that involves the coupling of the cold plasma X and O modes, and the kinetic EBWs. In the WKB limit, the EBW dispersion characteristics are related to the kinetic permittivity tensor element K_{xx}^K . In this limit, we retain all the cold plasma permittivity tensor elements except for the K_{xx} tensor element which is replaced by the corresponding kinetic tensor element obtained for a homogeneous, Maxwellian plasma⁸

$$K_{xx}^K = 1 + \frac{\omega_p^2}{\omega^2} \frac{y_0}{k_x^2 \rho^2} e^{-k_x^2 \rho^2} \sum_{n=-\infty}^{\infty} n^2 I_n(k_x^2 \rho^2) Z(y_n), \quad (4)$$

where $y_n = (\omega - n\omega_c)/(\sqrt{2}|k_{\parallel}|v_T)$, $\rho = v_T/\omega_c$ is the electron thermal Larmor radius, $v_T = \sqrt{\kappa T_e/m_e}$ is the electron thermal velocity corresponding to temperature T_e , $k_{\parallel} = (k_y B_{0y} + k_z B_{0z})/B_0$ is the component of \vec{k} along the magnetic field, I_n is the modified Bessel function of the first kind, and Z is the plasma dispersion function. We assume that, in the mode conversion region, $k_x \rho < 1$ and $y_n \gg 1$. The former approximation is valid since the wavelength of the EBW is comparable to that of the X mode in the mode conversion region. The latter approximation simply implies that there is no damping of waves in the mode conversion region; such a situation would be experimentally desirable. Consequently, on expanding the Bessel functions in (4) to second order in $k_x \rho$, and on keeping the leading term in the asymptotic form of the plasma dispersion function, we get

$$K_{xx}^K \approx 1 - \frac{\omega_p^2}{\omega^2 - \omega_c^2} + k_x^2 \rho^2 \left(\frac{\omega_p^2}{\omega^2 - \omega_c^2} - \frac{\omega_p^2}{\omega^2 - 4\omega_c^2} \right) \equiv K_{xx} + \chi_1 k_x^2, \quad (5)$$

where K_{xx} is given in (3). An inherent assumption in this expanded form of K_{xx}^K is that $\omega_{UH} < 2\omega_c$. When this is not the case, the character of the mode conversion region changes as the slow X mode propagates through the UHR towards the low density and low magnetic field part of the plasma. The conversion to EBW then occurs in a less dense plasma than in the case when the upper hybrid resonance frequency is less than $2\omega_c$. This is in contrast to the cold plasma result where the slow X mode asymptotes to zero perpendicular wavelength at the UHR. However, as discussed in Appendix A and Appendix B, the mode conversion formalism we develop here can be used in either case.

In order to appropriately convert the WKB result (5) to a unique operator form for a full wave description, proper attention must be given to total time-averaged energy flow conservation. The total time-averaged energy flow includes kinetic energy flow in addition to the electromagnetic (Poynting) energy flow. For a weakly damped kinetic wave, the time-averaged kinetic energy flow density is given by⁸

$$\langle \vec{s}_K \rangle = -\frac{1}{4} \epsilon_0 \omega \frac{\partial K_{\alpha\beta}^H}{\partial \vec{k}} E_{\alpha} E_{\beta}^*, \quad (6)$$

where we sum over repeated indices. α and β denote either the x , y , or z directions, E_{β}^* is the complex conjugate of E_{β} , and K^H is the Hermitian part of the kinetic permittivity tensor. With K_{xx} in (3) replaced by K_{xx}^K in (5), the kinetic energy flow density in the x direction is

$$\langle \vec{s}_K \rangle_x = -\frac{1}{4} \epsilon_0 \omega \frac{\partial K_{xx}^K}{\partial k_x} |E_x|^2. \quad (7)$$

For K_{xx}^K varying slowly with x , the conservation of the kinetic energy flow density

$$\frac{d}{dx} \left(\frac{\partial K_{xx}^K}{\partial k_x} |E_x|^2 \right) = 0 \quad (8)$$

requires that the inhomogeneous representation of the kinetic EBW mode be related to its homogeneous plasma representation $K_{xx}^K E_x$ by⁹

$$K_{xx}^K E_x \rightarrow K_{xx} E_x - \frac{d}{dx} \left(\chi_1 \frac{dE_x}{dx} \right). \quad (9)$$

So the approximate full-wave kinetic description of the EBW, coupled to the X and O modes, is included in Maxwell's equations (2), (3) by replacing $K_{xx} E_x$ on the right-hand side of (2) by the right-hand side of (9). With this replacement, Eqs. (2), (3) can be combined to give the following six coupled first order differential equations for the spatial evolution of the fields^{1,2}

$$\frac{d\vec{F}}{d\xi} = i\vec{A} \cdot \vec{F}, \quad (10)$$

where $\xi = \omega x/c$ is the normalized spatial variable,

$$\vec{F}^T = [E_x \ E_y \ E_z \ (i\tilde{\chi}_1 E_x)' \ cB_z \ (-cB_y)], \quad (11)$$

is the transpose of the field vector \vec{F} , $E_x' = (dE_x/d\xi)$, and

$$\vec{A} = \begin{bmatrix} 0 & 0 & 0 & -\tilde{\chi}_1^{-1} & 0 & 0 \\ n_y & 0 & 0 & 0 & 1 & 0 \\ n_z & 0 & 0 & 0 & 0 & 1 \\ K_{xx} & \chi_{xy} & \chi_{xz} & 0 & n_y & n_z \\ -\chi_{xy} & K_{yy} - n_z^2 & \chi_{yz} + n_y n_z & 0 & 0 & 0 \\ -\chi_{xz} & \chi_{yz} + n_y n_z & K_{zz} - n_y^2 & 0 & 0 & 0 \end{bmatrix}, \quad (12)$$

where $\tilde{\chi}_1 = (\omega/c)^2 \chi_1$, $n_y = ck_y/\omega$, and $n_z = ck_z/\omega$. The only component of the electromagnetic wave field whose evolution is not given by (10) is B_x . From (2)

$$cB_x = n_y E_z - n_z E_y. \tag{13}$$

Thus, the kinetic full-wave dynamics given by Eqs. (10)–(13) describe the coupling between the X mode, the O mode, and the EBW, i.e., the mode conversion process.

The total, electromagnetic and kinetic, time-averaged energy flow density in the x -direction is^{1,2}

$$\langle \vec{s} \rangle_x = \frac{1}{4} \sqrt{\frac{\epsilon_0}{\mu_0}} \vec{F}^\dagger \cdot \vec{R} \cdot \vec{F}, \tag{14}$$

where \vec{F}^\dagger is the transpose of the complex conjugate of \vec{F} and

$$\vec{R} = \begin{bmatrix} & & & 1 & 0 & 0 \\ & 0 & & 0 & 1 & 0 \\ & & & 0 & 0 & 1 \\ 1 & 0 & 0 & & & \\ 0 & 1 & 0 & & & 0 \\ 0 & 0 & 1 & & & \end{bmatrix}. \tag{15}$$

Then, from (10) we find that

$$\frac{d}{d\xi} (\vec{F}^\dagger \cdot \vec{R} \cdot \vec{F}) = 0. \tag{16}$$

This equation is needed to ensure that the numerical scheme solving the mode conversion equations is conserving the total, electromagnetic, and kinetic, time-averaged energy flow density. The conservation condition is consistent with the assumption that there is no damping in the mode conversion region; i.e., we assume that the EBW damping at the Doppler shifted electron cyclotron harmonic occurs inside the plasma away from the mode conversion region. For cases of interest this is verified by ray tracing of the EBW beyond mode conversion into the plasma.¹

The approximate kinetic dispersion relation, obtained by assuming WKB solutions of the form $e^{in_x \xi}$ in (10), is found to be

$$\det(n_x \vec{I} - \vec{A}) = 0, \tag{17}$$

where \det denotes the determinant.

III. GENERAL RELATIONSHIPS BETWEEN EMISSION AND EXCITATION COEFFICIENTS

In order to determine the scattering coefficients for mode conversion excitation of EBWs or for mode conversion emission from EBWs, Eqs. (10) are numerically solved (see Sec. IV) subject to boundary conditions discussed in Appendix B. While an analytical solution of these equations is essentially impossible for reasonable plasma parameters, relationships between the scattering coefficients for mode conversion excitation and the scattering coefficients for mode conversion emission can be established based on global properties of the model description. These relationships

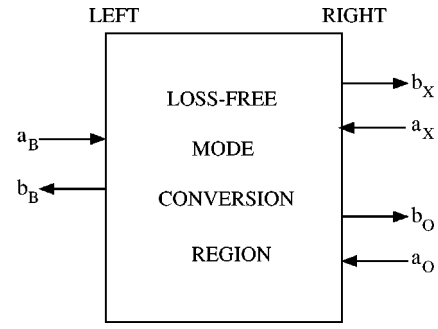


FIG. 1. The left-hand side is the high density region inside the plasma and the right-hand side is the low density region towards the outer part of the plasma. The indices X , O , and B label the X mode, O mode, and the EBW, respectively. a and b are complex amplitudes chosen such that $|a_i|^2 - |b_i|^2$ is the net wave energy flow density into the loss-free mode conversion region along the i th wave.

have to be satisfied by the results of any numerical procedure used to solve Eq. (10) with the appropriate boundary conditions.

The global properties of our full-wave model equations for the mode conversion region are linearity, energy flow conservation, and (Onsager-type¹⁰) time reversibility. From these properties we derive relationships between various mode conversion scattering coefficients. The derivation and the relationships apply to any full-wave description that has these global properties, and not just to the mode conversion process described by (10).¹¹

As explained in Appendix A, the wave fields are assumed to have a WKB form outside the mode conversion region. Referring to Fig. 1, towards the outside, low density region of the plasma (designated as “right”) the X and O modes are propagating with energy flow into or out of the mode conversion region, while the EBWs are evanescent with no associated energy flow. Towards the inside, high density region of the plasma (designated as “left”) the EBWs are propagating with energy flow into and out of the mode conversion region, while the X and O modes are evanescent with no energy flow. Let the complex amplitudes of the propagating modes be such that $|a_i|^2$ is the energy flow density into the mode conversion region and $|b_i|^2$ is the energy flow density out of the mode conversion region. ($i = X, O, B$ designating the X mode, the O mode, or the EBW, respectively.) Then, since the mode conversion equations are linear, the complex field amplitudes a_i and b_i are related by a scattering matrix

$$\begin{pmatrix} b_B \\ b_X \\ b_O \end{pmatrix} = \begin{pmatrix} S_B & S_{BX} & S_{BO} \\ S_{XB} & S_X & S_{XO} \\ S_{OB} & S_{OX} & S_O \end{pmatrix} \begin{pmatrix} a_B \\ a_X \\ a_O \end{pmatrix} \tag{18}$$

or, simply, in matrix notation

$$\vec{b} = \vec{S} \cdot \vec{a}. \tag{19}$$

The matrix \vec{S} is unique since the solution of the linear mode conversion equations with the appropriate boundary conditions (see Appendix B) is unique.

The requirement that the mode conversion region be free of dissipation implies that

$$\sum_i (|a_i|^2 - |b_i|^2) = 0. \quad (20)$$

Using (19), this conservation condition can be written as

$$\vec{a}^\dagger \vec{a} - \vec{a}^\dagger \cdot \vec{S}^\dagger \cdot \vec{S} \cdot \vec{a} \equiv \vec{a}^\dagger \cdot (\vec{I} - \vec{S}^\dagger \cdot \vec{S}) \cdot \vec{a} = 0, \quad (21)$$

where the dagger superscript denotes the complex conjugate of the transposed matrix. This condition must hold for any boundary conditions, i.e., for arbitrary \vec{a} . Consequently

$$\vec{S}^\dagger \cdot \vec{S} = \vec{I} \quad (22)$$

or

$$\vec{S}^\dagger = \vec{S}^{-1} \quad (23)$$

which is the constraint imposed on the elements of \vec{S} by the loss-free mode conversion process.

We next consider wave energy flow under time reversibility of the model dynamics. For the time reversed system the direction of time-averaged energy flow density changes sign. In other words, the reversal of time changes time-averaged energy flow *into* the mode conversion region to time-averaged energy flow *out* of the mode conversion region. This property for the electromagnetic part of the energy flow density requires that, under time reversal, the electric and magnetic fields change as follows:

$$\vec{E} \rightarrow \vec{E}^*, \quad \vec{B} \rightarrow -\vec{B}^* \quad (24)$$

and, for the kinetic part of the energy flow density, the wave vector changes according to

$$\vec{k} \rightarrow -\vec{k}. \quad (25)$$

(The complex conjugate variables are indicated by the superscript *.) In our description, a_i represents flow into the mode conversion while b_i represents flow out of the mode conversion region. Thus, if $a_i \sim \exp(ik_x x - i\omega t)$ then $b_i \sim \exp(-ik_x x - i\omega t)$. Consequently, under time reversal

$$a_i \rightarrow b_i^* \text{ and } b_i \rightarrow a_i^*. \quad (26)$$

Referring to Fig. 1, the effect of time reversal is to change a 's to b^* 's and b 's to a^* 's with arrows pointing in the same direction as indicated in the figure. Then, from the definition of the scattering matrix defined in (19)

$$\vec{a}^* = \vec{S} \cdot \vec{b}^*. \quad (27)$$

The complex conjugate of the above equation gives

$$\vec{a} = \vec{S}^* \cdot \vec{b}. \quad (28)$$

Then, from (19) and (28), energy flow under time reversibility imposes the constraint that

$$\vec{S}^* = \vec{S}^{-1}. \quad (29)$$

The relationship (29) along with (23) leads to the following property of the scattering matrix

$$\vec{S}^T = \vec{S}, \quad (30)$$

where the superscript T indicates the transpose of the matrix. Thus, the conservation of wave energy flow density, which follows from our assumption that the mode conversion region is free of any energy dissipation, and the requirement on energy flow under time reversibility lead to the conclusion that the scattering matrix \vec{S} is symmetric, i.e.,

$$S_{BX} = S_{XB}, \quad S_{BO} = S_{OB}, \quad S_{XO} = S_{OX}. \quad (31)$$

We can now evaluate the relationships between the emission and excitation coefficients. For this it is convenient to refer to Fig. 1. Let us first consider the excitation coefficients. If an X mode is launched from the right-hand side, low density region, then $a_O = 0$ and $a_B = 0$. From (18), it then follows that

$$\frac{b_B}{a_X} = S_{BX}. \quad (32)$$

The energy flow mode conversion coefficient for the excitation of EBW from an externally launched X mode is given by

$$C_{XB} = \left| \frac{b_B}{a_X} \right|^2 = |S_{BX}|^2. \quad (33)$$

Now let us consider the mode conversion of EBWs emitted from inside the plasma to the X mode towards the outside of the plasma. Here EBWs are incident on the mode conversion region from the high density, left-hand side, of the plasma. In this case $a_X = 0$ and $a_O = 0$. Then, from (18), we find that

$$\frac{b_X}{a_B} = S_{XB} = S_{BX}, \quad (34)$$

where we have used the condition (31) that \vec{S} is symmetric. The energy flow mode conversion coefficient for the emission of X mode from a thermally emitted EBW is then

$$E_X = \left| \frac{b_X}{a_B} \right|^2 = |S_{XB}|^2 = |S_{BX}|^2. \quad (35)$$

From (33) and (35) we note that $C_{XB} = E_X$, i.e., the fraction of the X mode energy flow that is mode converted to EBWs when an X mode is launched from the low density side is the same as the emitted EBW energy flow that is mode converted to an X mode that propagates out into the low density region. We can similarly show that $C_{OB} = E_O$, i.e., the fraction of the O mode energy flow that is mode converted to EBWs when an O mode is launched from the low density side is the same as the emitted EBW energy flow that is mode converted to an O mode that propagates out into the low density region. The emitted X and O modes propagate out into the vacuum region where they are observed in experiments.

In addition, from the symmetry of \vec{S} , it follows that

$$R_X \equiv |S_{OX}|^2 = |S_{XO}|^2 \equiv R_O, \quad (36)$$

i.e., for an X mode launched from the outside, the fraction of the X mode energy flow that is reflected back out on the O mode is the same as the fraction of the O mode energy flow that is reflected back out on the X mode for an O mode launched from the outside.

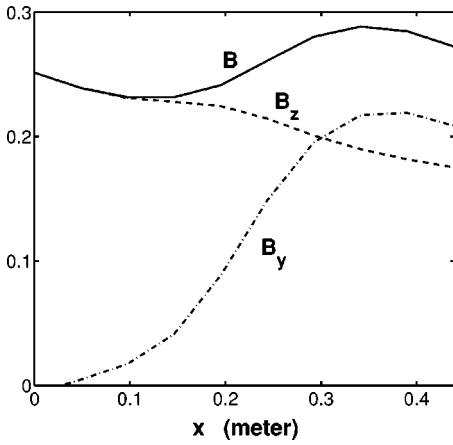


FIG. 2. The magnitudes of the poloidal component B_y (dotted-dashed), the toroidal component B_z (dashed), and the total magnetic field B (solid line) in Tesla as a function of the minor radius. $x=0$ is the center of the plasma and $x=0.44$ m is the outside edge of the plasma.

So, in summary, the symmetry of the scattering matrix \vec{S} leads to the following relationships that have important experimental consequences

$$E_X = C_{XB}, \quad E_O = C_{OB}, \quad R_X = R_O. \quad (37)$$

IV. EXCITATION AND EMISSION OF ELECTRON BERNSTEIN WAVES

The kinetic field equations in (10) are solved numerically with the boundary conditions discussed in Appendix B. The NSTX-type high- β equilibrium that we have used in our calculations is as follows.¹ The Shafranov-shifted major radius is $R=1.05$ m, the minor radius is $a=0.44$ m, the peak electron density is $n_0=3 \times 10^{19} \text{ m}^{-3}$, the peak electron temperature is $T_0=3$ keV, the density profile is $n_e = n_E + (n_0 - n_E)(1 - x^2/a^2)^{1/2}$, and the temperature profile is $T_e = T_E + (T_0 - T_E)(1 - x^2/a^2)^2$, where n_E and T_E are the edge density and temperature, respectively, with $n_E/n_0=0.02$ and $T_0/T_E=0.02$. The magnetic field profile is taken to be that shown in Fig. 2.

For a wave frequency of 14 GHz, Fig. 3 shows the energy flow mode conversion efficiency C_{XB} for the excitation of EBWs when an X mode is launched from outside the

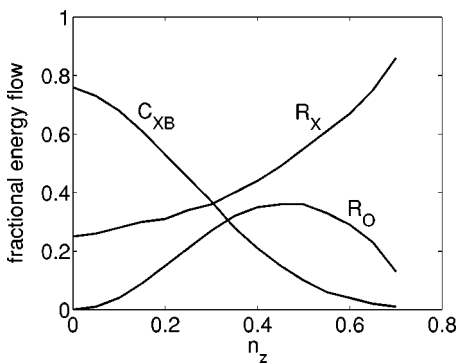


FIG. 3. The fraction of the incoming X mode energy flow, as a function of n_z for $k_y=0$, that is reflected out on the X mode R_X , on the O mode R_O , and mode converted to Bernstein waves C_{XB} .

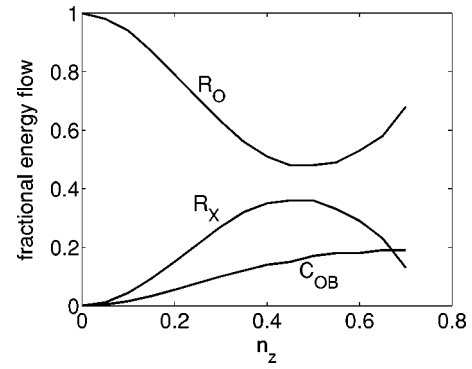


FIG. 4. The fraction of the incoming O mode energy flow, as a function of n_z for $k_y=0$, that is reflected on the X mode R_X , on the O mode R_O , and mode converted to Bernstein waves C_{OB} .

plasma. In this case the upper hybrid frequency is below $2\omega_c$. Figure 4 shows the mode conversion efficiency C_{OB} when, for the same parameters, an O mode is launched from the outside.

When EBWs are emitted, they propagate out to the edge where they can couple to the X and O modes near the UHR. Some of the EBW energy flow reaching the UHR will be reflected back into the plasma. For the same parameters as discussed above, Fig. 5 shows the fraction of the emitted EBW energy flow, as a function of k_z , that is converted to the X mode E_X , to the O mode E_O , and reflected back into the plasma R_B . Upon comparing the results from Figs. 3 and 4 with those given in Fig. 5 we note the following relationships:

$$E_X = C_{XB} \quad \text{and} \quad E_O = C_{OB}. \quad (38)$$

These are exactly the same conditions as derived in Sec. III. Thus, the fraction of the EBW emitted energy flow that is mode converted to the X mode and the O mode is the same as the energy flow that is mode converted from the X mode to the EBW when the X mode is launched from the outside, and, separately, from the O mode to EBW when the O mode is launched from the outside.

Since $E_X + E_O \leq 1$, it follows that if the plasma conditions are such that the X-B conversion process is optimized then the O-B conversion process is not effective, and vice

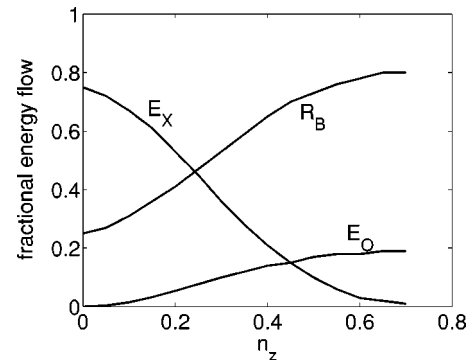


FIG. 5. The fraction of the outgoing EBW energy flow, as a function of n_z for $k_y=0$, that is converted to the X mode E_X and to the O mode E_O . R_B is the fraction of the emitted EBW energy flow that is reflected back into the plasma.

versa. We have noted this effect before when studying the mode conversion excitation of EBWs.¹ It was found that the $X-B$ and the $O-B$ conversion processes were optimized in, essentially, mutually exclusive regions of the parameter space spanned by (ω, k_{\parallel}) (where k_{\parallel} is the component of \vec{k} parallel to \vec{B}_0). Consequently, from the relationships in (38) we can conclude that the experimental design for the excitation of EBWs can be completely based on the EBW emission characteristics of the plasma. For example, plasma edge conditions that give a maximum of EBW emission received externally in the X mode will also be optimum for obtaining maximum mode conversion to EBW propagating into the plasma from an externally excited X mode.

From Figs. 4 and 3, respectively, we also note

$$R_X = R_O, \quad (39)$$

exactly as predicted in Sec. III.

V. CONCLUSIONS

We have developed an approximate kinetic model for studying the energy flow transfer between the X mode, the O mode, and the EBW in the mode conversion region in the vicinity of the cold plasma upper hybrid resonance. This model explicitly includes the propagation of EBWs so that we can correctly account for the kinetic energy flow on the EBWs. This is in contrast to the cold plasma models where the resonance absorption at the UHR is treated to be equivalent to the energy flow mode converted to EBWs.¹

We assume that there is no dissipation of energy within the mode conversion region. This assumption is not a matter of convenience. If heating and current drive by EBWs is to be achieved in the high density region of spherical tokamak plasmas, the damping region has to be spatially separated from the, relatively low density, mode conversion region. Then, from general considerations of energy flow conservation and energy flow under time reversal, we have shown that the emission coefficients are the same as the excitation coefficients. For the same plasma parameters and wave parameters, the excited energy flow that would be mode converted to EBWs when an X mode is launched from the outside is the same as the energy flow emitted on the X mode from EBW emission inside the plasma. Similarly, the excited energy flow that would be mode converted to EBW when an O mode is launched from the outside is the same as the energy flow that is emitted on the O mode from EBW emission inside the plasma. The solutions for the wave fields obtained from numerical integration of the approximate kinetic model verify the global symmetry results obtained analytically.

The relationship between emission and excitation coefficients has an interesting implication. By itself, the cold plasma resonance absorption model cannot be used to evaluate, directly, the energy flow that is mode converted to the X mode and the O mode from EBW emission. That is because the cold plasma model does not include EBWs. However, general analytical results and numerical results from the approximate kinetic model show that the resonance absorption model can be used to determine the emission coefficients. All

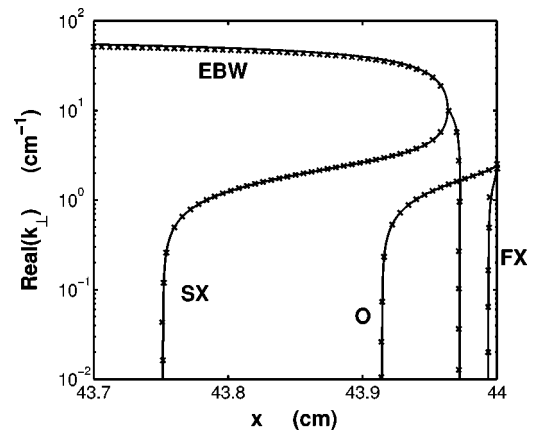


FIG. 6. The dispersion characteristics for the X mode, O mode, and the EBW for NSTX-type parameters for a wave frequency of 14 GHz. In this case the upper hybrid frequency is below the second harmonic of the electron cyclotron frequency. The cold plasma upper hybrid resonance is located at $x \approx 43.97$ cm. The solid lines are the characteristics obtained from the fully kinetic (Maxwellian) plasma dispersion relation. The crosses mark the characteristics obtained from the approximate kinetic dispersion relation (17).

we need to do is to evaluate C_{XB} and C_{OB} , the $X-B$ and the $O-B$ excitation coefficients, respectively, for the same wave and plasma parameters. Then the emission coefficients E_X and E_O , for emission of the X and O modes, respectively, are equal to the corresponding excitation coefficients. Since the sum of the two emission coefficients $E_X + E_O$ has to be less than, or equal to, unity, the sum of the two excitation coefficients $C_{XB} + C_{OB}$ has also got to be less than, or equal to, unity. The difference from unity of the sum $E_X + E_O = C_{XB} + C_{OB}$ is the fraction of the emitted EBW energy flow that is reflected back into the plasma from the mode conversion region.

The inequality $C_{XB} + C_{OB} \leq 1$ also implies that the two mode conversion processes, $X-B$ and $O-B$, are complementary to each other. If, for a given plasma configuration, the wave parameters are chosen to maximize one particular mode conversion process then the other conversion process will be minimized. This has been noticed in our earlier mode conversion studies pertaining to the excitation of EBWs from X mode or O mode.¹ The two mode conversion processes are optimized in completely different parts of the parameter space spanned by the parallel (to the magnetic field) wave numbers and wave frequency.¹

The equality between the emission coefficients and the excitation coefficients also points to the fact that optimized mode conversion heating and current drive experiments can be designed on the basis of the emission results. The conditions for which the X mode (or the O mode) emission is most pronounced will be the conditions for which the $X-B$ (or the $O-B$) mode conversion is optimized.

ACKNOWLEDGMENTS

This work was supported by Department of Energy Contracts Nos. DE-FG02-91ER-54109 and DE-FG02-99ER-54521, and partially by the UK Department of Trade and Industry and EURATOM. One of us (A.K.R.) would like to

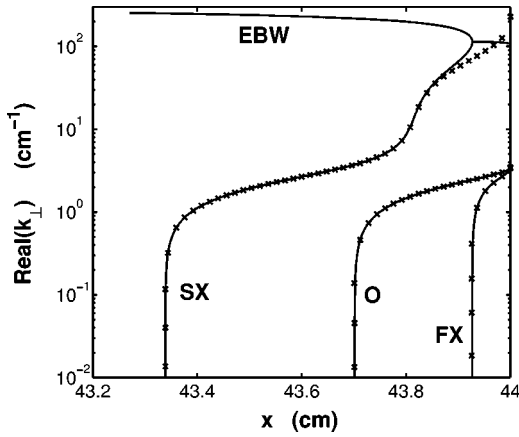


FIG. 7. Same as Fig. 6 except that the wave frequency is 18 GHz (corresponding to the upper hybrid frequency being greater than twice the electron cyclotron frequency). The cold plasma upper hybrid resonance is located at $x \approx 43.8$ cm.

thank Dr. Jack Connor and the theory staff for the hospitality provided at the Culham Science Center where part of this work was carried out, and to UKAEA for providing travel support.

APPENDIX A: LOCAL DISPERSION CHARACTERISTICS

As mentioned in the text of the paper, the approximate WKB dispersion relation obtained in (17) does not describe the EBW branch of the dispersion relation when the upper hybrid frequency is greater than $2\omega_c$.

For the case when the upper hybrid frequency is less than $2\omega_c$, Fig. 6 shows a comparison of the dispersion characteristics obtained from (17), marked by crosses, with those obtained from the exact kinetic (Vlasov–Maxwell), Maxwellian plasma description.¹² Any differences between the characteristics of the waves between the two cases are essentially indistinguishable. The parameters used here are NSTX type¹ and the wave frequency is 14 GHz. Figure 7 shows the comparison for the case when the wave frequency is 18 GHz and the upper hybrid frequency is larger than $2\omega_c$. The matching between the two dispersion relations is good except where the slow X mode couples to the EBW. In the approximate model of (17), the slow X mode continues to propagate out to the edge of the plasma while the complete description gives a coupling between the slow X mode and the EBW. This shows that a description containing terms higher than second order in the Larmor radius are needed. However, for the purposes of our studies on mode conversion excitation and emission, we note that this is not necessary. From the exact description, in the region to the right (low density) of the SX-EBW coupling the two modes are evanescent. Any energy flow transferred to the SX mode in the higher density region will propagate outwards towards the low plasma density region and then fully convert to the EBW. There are no other waves that are involved in this SX-EBW coupling process and neither of the two modes are cutoff. So, we postulate that, in our approximate description of the mode conversion process, any energy flow coupled to

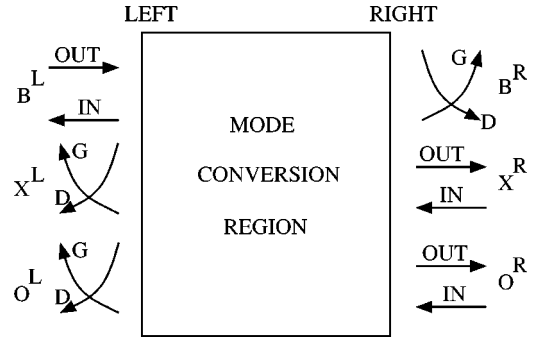


FIG. 8. Boundary conditions for $\omega_{UH} < 2\omega_c$. The EBW is indicated by the letter *B*. The arrows indicate the direction of the energy flow density. The other labels are, respectively, as follows: *G* and *D* represent exponentially growing and decaying modes, *L* and *R* represent the left (high density) and right (low density) boundaries, and IN and OUT indicate the inward and outward propagating waves. The boundary conditions are specified as follows. (a) For emission set $B_{OUT}^L = 1$, $X_G^L = 0$, and $O_G^L = 0$. Then (10) is solved for B_{IN}^L , X_D^L , and O_D^L such that $B_G^R = 0$, $X_{IN}^R = 0$, and $O_{IN}^R = 0$. This procedure then determines B_D^R , X_{OUT}^R , and O_{OUT}^R . (b) For mode conversion when only the X mode is incident from the right boundary set $B_{OUT}^L = 0$, $X_G^L = 0$, and $O_G^L = 0$. Then (10) is solved for B_{IN}^L , X_D^L , and O_D^L such that $B_G^R = 0$, $X_{IN}^R = 1$, and $O_{IN}^R = 0$. This procedure determines B_D^R , X_{OUT}^R , and O_{OUT}^R .

the SX mode for the case when the upper hybrid frequency is larger than $2\omega_c$ will be coupled to the EBW. Or, conversely, any EBW energy flow propagating out towards the low density side will fully convert to the SX mode at the position where these two modes couple, i.e., where the SX and EBW branches coalesce in $\text{Re}(k_{\perp})$. It is important to note that, in this case, as the SX mode propagates towards the high density side it reaches the high-density cutoff. At this point energy will be reflected back onto the SX mode propagating towards the low density side. This, however, is taken into account in our approximate full-wave kinetic description. With this argument in mind, we describe in Appendix B the appropriate boundary conditions imposed on the set of Eqs. (10) for mode conversion and emission studies.

APPENDIX B: BOUNDARY CONDITIONS IN THE SOLUTION OF EQ. (16)

For numerical studies of EBW emission, or EBW excitation by mode conversion, the system of Eqs. (10) is solved with the boundary conditions described below. In the following it is helpful to refer to Figs. 6 and 7.¹³ When we mention the left boundary, it implies the boundary in the plasma in the high density region, while the right boundary is the low density edge region of the plasma. In addition, outgoing and incoming refers to propagating waves with their energy flow density towards the low density and the high density regions, respectively. The left boundary (at high densities, “inside”) and the right boundary (at low densities, “outside”) are taken to be away from the mode conversion region where the perpendicular wave vectors, obtained from the WKB dispersion relation, change slowly compared to the density scale length. Then, at the two boundaries, the six waves are assumed to be independent and uncoupled, and the solutions to Eq. (10) are obtained using the WKB approximation. For emission of EBWs from inside the plasma, or for mode con-

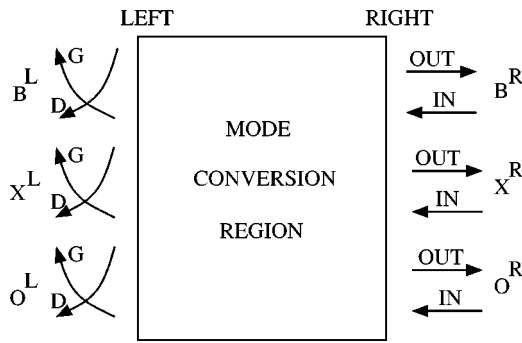


FIG. 9. Same as Fig. 8. Boundary conditions for $\omega_{UH} > 2\omega_c$ are specified as follows. (a) For emission set $B_G^L=0, X_G^L=0,$ and $O_G^L=0$. Then (10) is solved for $B_D^L, X_D^L,$ and O_D^L such that $B_{IN}^R=1, X_{IN}^R=0,$ and $O_{IN}^R=0$. This procedure then determines $B_{OUT}^R, X_{OUT}^R,$ and O_{OUT}^R . (b) For mode conversion when the X mode is incident from the right boundary set $B_G^L=0, X_G^L=0,$ and $O_G^L=0$. Then (10) is solved for $B_D^L, X_D^L,$ and O_D^L such that $B_{IN}^R=0, X_{IN}^R=1,$ and $O_{IN}^R=0$. This procedure determines $B_{OUT}^R, X_{OUT}^R,$ and O_{OUT}^R .

version excitation of EBWs from outside the plasma, we consider the two cases when the upper hybrid frequency is either less than or greater than $2\omega_c$.

1. Emission of EBW

For the upper hybrid frequency less than $2\omega_c$, the WKB solutions at the left boundary correspond to incoming and outgoing EBWs, and to X and O modes that are spatially (exponentially) decaying and growing. The WKB solutions at the right boundary correspond to incoming and outgoing X and O modes, and EBW modes that are spatially decaying and growing as a function of distance out of the plasma. At the left boundary, the field amplitudes of the spatially growing X and O modes are set to zero, and the energy flow on the outgoing EBW is normalized to unity. Then the field amplitudes of the incoming EBW and of the spatially decaying X and O modes, at the left boundary, are chosen in such a way that, at the right boundary, the field amplitudes of the incoming X and O modes, and of the spatially growing EBW wave are zero. With these boundary conditions we determine, at the right boundary, the outgoing energy flow on the X and O waves, and the field amplitude of the decaying EBW. This is illustrated and summarized in Fig. 8(a).

For the upper hybrid frequency greater than $2\omega_c$, the WKB solutions (Fig. 7, cross marks) at the left boundary correspond to $X, O,$ and EBW modes that are spatially decaying and growing. At the right boundary the WKB solutions correspond to incoming and outgoing X modes, O modes, and EBWs. In our approximate kinetic analysis, as discussed in the text and in Appendix A, the propagating EBWs are just an extension of the SX mode as it propagates through the cold plasma UHR. So the EBW with energy flowing outwards is the one that is effectively carrying energy into the plasma for the fully kinetic dispersion relation. And the EBW with energy flowing inwards (towards the SX cutoff) is the one that is effectively carrying energy outward from the core in the fully kinetic dispersion relation. At the left boundary, the amplitudes of the three spatially growing modes are set identically to zero while the amplitudes of the

spatially decaying modes are chosen to be such that, at the right boundary, there is no energy flow on the incoming X and O modes, and the energy flowing inward on the EBW is unity. With these boundary conditions, we find, at the right boundary, the energy flow on the outgoing EBW and the outgoing X and O modes for unit energy flow on the incoming EBW. This is illustrated and summarized in Fig. 9(a). Note that B_{IN}^R is taken as effectively the EBW from inside the plasma with energy flow toward the outside; B_{OUT}^R is effectively the EBW energy flow reflected from the mode conversion region and flowing into the plasma.

2. Mode conversion excitation of EBW

When considering mode conversion to EBWs from externally launched X mode or externally launched O mode, we set up the boundary conditions as follows. Let us consider the case of an externally launched X mode; for an externally launched O mode the appropriate boundary conditions can be easily determined by analogy.

For the case when the upper hybrid frequency is less than $2\omega_c$, at the left boundary, the amplitudes of the spatially growing X and O modes are set to zero, and the amplitude of the outgoing EBW is set to zero. Then the amplitudes of the spatially decaying X and O modes, and the ingoing EBW, at the left boundary, are determined by the requirement that, at the right boundary, the incoming X mode energy flow density is unity, and the field amplitudes of incoming O mode and the spatially growing EBWs are zero. Then, upon solving (10), we find the outgoing energy flow on the X and O modes, and the amplitude of the spatially decaying EBW at the right boundary [see Fig. 8(b)]. Thus, this determines the energy flow mode converted from an X mode, for no incoming energy flow on the O mode, and the reflected energy flow coming out on both the X mode and the O mode.

For the case when the upper hybrid frequency is greater than $2\omega_c$, the amplitudes, at the left boundary, of the spatially growing X mode, O mode, and EBW are set to zero. The field amplitudes, at the left boundary, of the spatially decaying X mode, O mode, and EBW, are obtained such that, at the right boundary, the energy flow in the incoming X mode is unity, and the field amplitudes of the incoming O mode and the incoming EBW are zero. Then, upon solving (10), we find, at the right boundary, the energy flow on the outgoing X and O modes and the energy flow mode converted to the outgoing EBW [see Fig. 9(b)]. Note that B_{OUT}^R is taken as effectively the energy flow mode converted from an externally excited X mode, and X_{OUT}^R and O_{OUT}^R are the reflected energy flows coming out on the X and O modes, respectively.

¹A. K. Ram and S. D. Schultz, Phys. Plasmas **7**, 4084 (2000).
²A. Bers, A. K. Ram, and S. D. Schultz, in *Proceedings of the Second Europhysics Topical Conference on RF Heating and Current Drive of Fusion Devices*, edited by J. Jacquinot, G. Van Oost, and R. R. Weynants (European Physical Society, Petit-Lancy, 1998), Vol. 22A, pp. 237–240.
³J. Preinhaelter and V. Kopecky, J. Plasma Phys. **10**, 1 (1973).
⁴H. P. Laqua and H. J. Hartfuss, Phys. Rev. Lett. **81**, 2060 (1998).
⁵B. Jones, G. Taylor, P. C. Efthimion, T. Munsat, J. C. Hosea, R. Kaita, R. Majeski, and J. Menard, Bull. Am. Phys. Soc. **45**, 344 (2000).

⁶V. Shevchenko, G. Cunningham, and A. Field, in *Abstracts of Invited and Contributed Papers, 28th European Physical Society (EPS) Conference on Controlled Fusion and Plasma Physics*, edited by C. Silva, C. Varandas, and D. Campbell (European Physical Society, Petit-Lancy, 2001), p. 381; (<http://www.cfn.ist.utl.pt/EPS2001/fin/pdf/p3.101.pdf>).

⁷P. K. Chattopadhyay, J. K. Anderson, T. M. Biewer, C. B. Forest, and M. Thomas, *Bull. Am. Phys. Soc.* **45**, 110 (2000).

⁸See, for example, W. P. Allis, S. J. Buchsbaum, and A. Bers, *Waves in Anisotropic Plasmas* (Massachusetts Institute of Technology Press, Cambridge, MA, 1963), Sec. 8.5; A. Bers, in *Plasma Physics—Les Houches 1972*, edited by C. DeWitt and J. Peyraud (Gordon and Breach, New York, 1975), pp. 126–137; and T. Stix, *Waves in Plasmas* (American Institute of Physics, New York, 1992), pp. 74–78.

⁹H. Berk and D. L. Book, *Phys. Fluids* **12**, 649 (1969).

¹⁰The usual Onsager relationships are based upon the transformation of

phase space dynamics and real fields under time reversibility; in this paper, in (\vec{k}, ω) space and for complex amplitude fields, we consider the transformation of time-averaged energy flow under time reversibility.

¹¹A. Bers and A. K. Ram, “General proof of symmetries in mode conversions,” *Bull. Am. Phys. Soc.* (in press).

¹²The exact kinetic dispersion relation is $\det(\vec{n}\vec{n} - \vec{n} \cdot \vec{n} \vec{I} + \vec{K}) = 0$ where $\vec{n} = c\vec{k}/\omega \equiv (n_x, n_y, n_z)$ and \vec{K} is the exact kinetic permittivity tensor (Ref. 8).

¹³It should be noted that, unlike the X and O modes, the EBW is a backward wave, i.e., its group velocity is in the opposite direction to its phase velocity. The dispersion characteristics in Figs. 6 and 7 are symmetric about $\text{Re}(k_\perp) = 0$. Hence, the direction, in x , of the wave energy flow for the designated waves must be associated, as appropriate, with positive or negative $\text{Re}(k_\perp)$.